Textures and Microstructures, Vol. 30, pp. 191–206
Reprints available directly from the publisher
Photocopying permitted by license only

© 1998 OPA (Overseas Publishers Association) N.V.
Published by license under
the Gordon and Breach Science
Publishers imprint.
Printed in India.

AN INVESTIGATION ON GRAIN GROWTH IN A COMMERCIAL Al–Mg ALLOY

I. SAMAJDAR[a,*], L. RABET[b], B. VERLINDEN[a] and P. VAN HOUTTE[a]

[a]*Department MTM, Katholieke Universiteit Leuven, de Croylaan 2, 3001 Heverlee, Belgium;* [b]*Royal Military Academy, Brussels, Belgium*

(Received 5 August 1997)

Alloy AA5182 contains coarse constituent particles and submicron dispersoids. While the former may cause particle stimulated nucleation (PSN) during primary recrystallization, the fine dispersoids may 'arrest' grain growth during subsequent annealing. Abnormal grain growth was observed after dissolution/coarsening of the dispersoids. Mainly S [{123}⟨634⟩] grains, but also some Brass [{011}⟨112⟩] and Cu [{112}⟨111⟩] grains, were observed to grow abnormally. Both the grain size and the grain boundary character distribution (GBCD) possibly played a role in the selection of the grains for abnormal grain growth. A dramatic increase in the number fraction of extremely low angle (1–5°) boundaries was observed with annealing, the increase being more at 470°C (when dispersoids were stable and grain growth was arrested more effectively) than at 500°C/530°C (when inhibition to grain growth was less). The nature of the CSL boundaries did not change significantly with annealing time/temperature.

Keywords: AA5182; Particle pinning; Grain growth; Grain boundary character distribution; Coincidence site lattice boundary

INTRODUCTION

Grain boundaries can be characterized by the misorientation, using the usual axis–angle pair (Randle, 1992), and also by the coincidence site lattice (CSL) (Smith and Pond, 1976; Randle, 1992). Relative frequencies of grain boundary types (the so-called grain boundary character distribution (GBCD) (Watanabe, 1992) or Mesotexture (Randle, 1992) may provide crucial information on the structure–property

* Corresponding author. Fax: (+32) 16 321992.

TABLE I Weight percentages of the major alloying elements in AA5182

Si	*Fe*	*Mn*	*Mg*
0.15	0.32	0.29	4.3

relationships and several attempts have been made to understand and to control it – Randle and Brown (1989), Watanabe *et al.* (1989), Palumbo *et al.* (1991), Watanabe (1992), Chiba *et al.* (1994), Hayakawa *et al.* (1997). Grain growth is often considered to affect the frequencies of different types of grain boundaries (Randle and Brown, 1989; Watanabe *et al.*, 1989; Humphreys and Hatherly, 1995) and may be used as a tool for the GBCD control. The frequencies of low energy boundaries (such as low angle boundaries and low Σ boundaries) are expected (Humphreys and Hatherly, 1995), and were experimentally observed (Randle and Brown, 1989; Watanabe *et al.*, 1989), to increase with grain growth. However, our understanding of the effects of annealing and grain growth (especially when it may involve particle coarsening/dissolution) on the GBCD in commercial alloys is far from complete.

In the present study, an effort will be made to outline change(s) in grain sizes and GBCD of a commercial Al–Mg–Mn alloy of type AA5182 (for details on chemical composition see Table I), as a function of annealing times and for 470°C, 500°C and 530°C annealing. The microstructure of this alloy is characterized by a large amount of submicron dispersoids with an average size of 0.2 μm and a spacing of 1–3 μm, and by coarse constituent particles with an average size of 5.6 μm and an average interparticular spacing of 12 μm (Ratchev *et al.*, 1995; Rabet, 1996). While some of the dispersoids, potential causes for grain boundary pinning, may get dissolved at and above 500°C, the constituent particles are stable for the range of grain growth temperatures used in this study (Ratchev *et al.*, 1995; Rabet, 1996). Abnormal grain growth, initiated by the dissolution/coarsening of the dispersoids, was also studied in terms of global textural changes and possible 'selection' mechanisms (selecting or favoring grains of certain orientations).

EXPERIMENTAL METHODS

The alloy AA5182 was obtained in as cold-rolled condition (rolling strain of $\varepsilon = 1.2$) from Hoogovens Aluminium. The submicron

dispersoids are present as rhombohedral and platelike particles and the former are expected to dissolve at and above 500°C (Ratchev *et al.*, 1995). The cold-rolled material was annealed at 470°C, 500°C and 530°C in a salt bath. Full recrystallization at these temperatures was observed to take only 1–5 s (Rabet, 1996; Samajdar *et al.*, 1997). Subsequently after annealing, the macroscopic texture was measured by X-ray diffraction using the software MTM-FHM (Van Houtte, 1995). This software uses the standard series expansion method (Bunge, 1982).

Measurements of microtexture and grain boundary characterizations were obtained by Orientation Imaging Microscopy (OIM) on surfaces containing rolling (RD) and normal (ND) directions, using the standard TSL™ OIM software. For OIM measurements, *at least* (and often more) an area of 1000 μm by 200 μm was used. CSL boundaries were identified using Brandon's criteria (Brandon, 1966), i.e. CSL tolerance being $15°/\Sigma^{0.5}$. Grains were *identified* as regions without >1° boundaries inside, as 0–1° relative misorientations were considered within the tolerance of the OIM measurements. Area and number fractions of such >1° misoriented regions were measured by OIM and grain size distributions were calculated by assuming circular grains with $\pi d^2/4$ as area, where d is the equivalent grain diameter (or the grain size). OIM measurements of grain sizes were further confirmed by measurements using the standard linear intercept technique. Constituent particles were identified from the low confidence index of the measurements and were substantiated by backscattered electron imaging in SEM. For grain size and GBCD measurements, points with low confidence index (i.e. unsolvable patterns, or when the beam did strike second phase particles) were filtered out. Both the total number and the number of different types of grain boundaries (as seen in linear scans) were estimated and the grain boundary types were represented as corresponding number fractions. Details of the OIM sample preparation is described elsewhere (Samajdar *et al.*, 1997).

RESULTS

I. Changes in Grain Size with Annealing

Figure 1 plots the grain sizes as a function of the natural logarithm of the annealing time (in s) and for 500°C annealing. The material

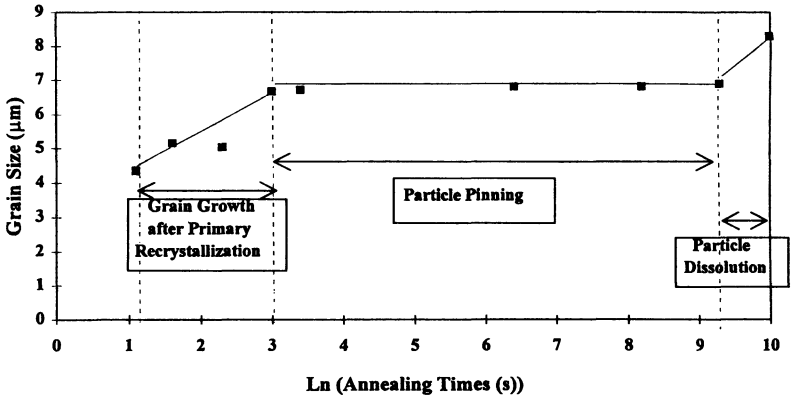

FIGURE 1 Grain size as a function of annealing times (s) (logarithmic scale) for annealing at 500°C.

recrystallized fully after 3 s annealing with an average grain size of 4.35 μm. Further annealing to 20 s was observed to increase the average grain size to 6.7 μm. Between 20 and 10 800 s, the average grain size did not change much. Further increases in grain sizes were observed only at and above 21 600 s. Annealing at 470°C or 530°C provided similar 'limiting' grain sizes of approximately 7 μm. At 470°C, no subsequent grain growth was observed (i.e. after reaching the limiting grain size), while grain growth was observed at and above 10 800 s for 530°C annealing. Qualitative observations using backscattered electron imaging on the electropolished samples showed no significant change in particle distribution (especially for the visible fine dispersoids) at 470°C. With prolonged heating at relatively higher temperatures (10 800 s at 500°C and 3600 s at 530°C), however, interparticle spacings of the fine dispersoids were observed to increase. As the dispersoids are considered (Ratchev *et al.*, 1995; Rabet, 1996) to be mainly responsible for the grain boundary pinning, changes in dispersoid spacings may explain the observed subsequent (i.e. after reaching the limiting grain size) grain growth at 500°C/530°C and no apparent grain growth at 470°C.

II. Changes in GBCD with Annealing

An effort was also made to characterize the possible change(s) in GBCD during annealing. Figure 2(a) plots the number fraction of

grain boundaries as a function of misorientation angle, for different annealing times at 470°C. Figure 2(a) starts with annealing time of 30 s, as before 30 s changes in GBCD were relatively less significant and no distinct trend could be established. Grain boundary misorientations were considered from 1° to 62.8°, as boundaries between 0° and 1° are within the tolerance of the OIM measurements. The frequencies of grain boundaries in random textured material (Samajdar and Doherty, 1994) are also plotted in the figure. As shown in the figure, although the grain size did not change significantly after 30 s, prolonged annealing at 470°C *increased* the fraction of extremely low angle (1–5°) boundaries – an increase from 0.014 to 0.11, as annealing time increased from 30 to 21 600 s. Note that after reaching a relative maxima of approximately 0.11 (as in Fig. 2(a)), the fraction of 1–5° boundaries did not increase further with subsequent annealing.

The initial misorientation distributions were similar (i.e. after 30 s annealing at 470°C, 500°C and 530°C) and qualitatively similar changes (as in Fig. 2(a)) were observed during annealing at 500°C and 530°C. In other words, the fractions of extremely low angle 1–5° boundaries were observed to reach an approximate maxima and then roughly stabilize for all three annealing temperatures. Although at 470°C grain growth was effectively 'arrested' above 30 s annealing, grain growth (in the form of noticeable increase in average grain size) was observed at and above 21 600 and 10 800 s for 500°C and 530°C annealing respectively. Interestingly, the initiation of such grain growth did not *change* the relative maxima of 1–5° boundaries. Figure 2(b) plots the grain

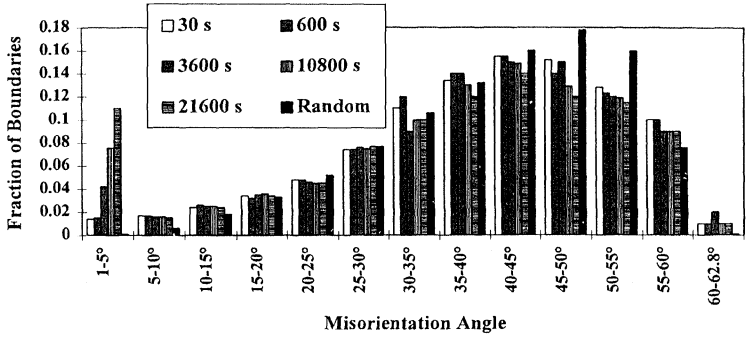

FIGURE 2(a) Fraction of boundaries as a function of misorientation angle for 470°C annealed material.

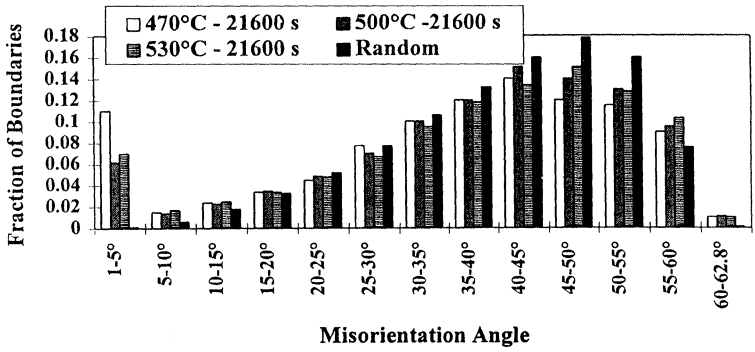

FIGURE 2(b) Fraction of boundaries as a function of misorientation angle after 21 600 s annealing at 470°C, 500°C and 530°C.

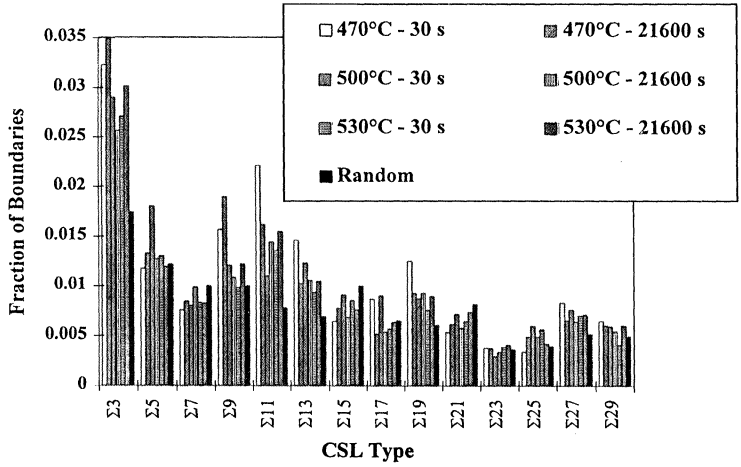

FIGURE 3 Fraction of CSL boundaries after different annealing treatments.

boundary fractions (as function of misorientation angle and using the same conventions as in Fig. 2(a)) after 21 600 s annealing at 470°C, 500°C and 530°C. Interestingly enough, the fraction of extremely low angle (1–5°) boundaries were larger after annealing at 470°C (when the grain growth was largely restricted) than at 500°C/530°C (when limited grain growth was observed).

Figure 3 plots the number fraction of CSL boundaries (Σ3–Σ29) after different annealing treatments. Fraction of CSL boundaries

expected in a random structure (Watanabe, 1992) are also marked on the figure. As shown in Fig. 3, the nature of the CSL boundaries (both in terms of the total fraction and also for particular CSL types) did not change significantly with annealing time/temperature. Number fraction of grain boundaries (both in terms of misorientation and CSL fraction) were calculated from two OIM scans of 1000 μm by 200 μm in each sample and average values of such boundary fractions are reported in Figs. 2 and 3.

III. Abnormal Grain Growth

III(a). Changes in Bulk Texture

X-ray texture results were analyzed using orientation distribution functions (ODF) (Bunge, 1982). Volume fractions for different orientations were measured from X-ray ODFs by convoluting with appropriate model functions, where the model functions had a maximum integrated ODF value of 1 and used a Gaussian spread of 16.5° (Van Houtte, 1995). No *significant* textural changes (and also no apparent abnormal grain growth) were observed during 470°C annealing. During 500°C or 530°C prolonged annealing, however, a considerable increase in rolling texture components was observed. Figure 4 plots the volume fractions of Goss [{011}⟨100⟩], Brass [{011}⟨112⟩],

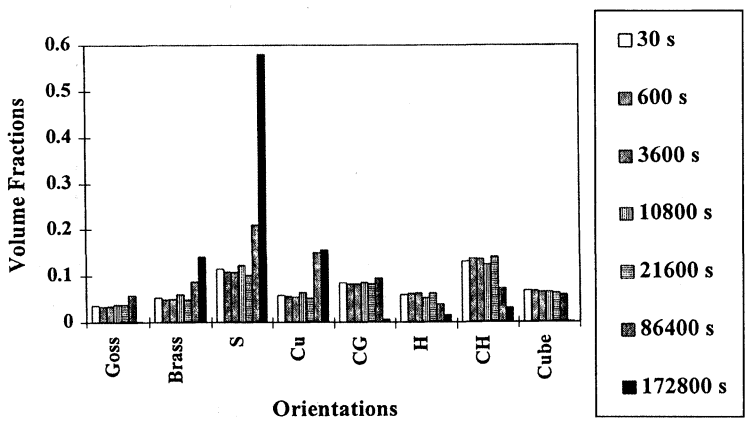

FIGURE 4 Volume fractions of different orientations as a function of annealing times (530°C annealing).

S [{123}⟨634⟩], Cu [{112}⟨111⟩] and CG [{012}⟨110⟩] (all of which belong to the usual fcc rolling texture) and also for Cube [{001}⟨100⟩], H [{001}⟨110⟩] and CH [{001}⟨120⟩] (the last two belonging to the potential PSN orientations) (Rabet, 1996; Samajdar *et al.*, 1997), as function of annealing times (in s, for 530°C annealing). As shown in the figure, till 21 600 s annealing the volume fractions of individual orientations do not change noticeably. Above 21 600 s, marked increase in rolling texture orientations (especially for S) did coincide with significant abnormal grain growth. Observed textural changes on the X-ray ODFs were further substantiated by OIM scans.

III(b). Selection Mechanisms

OIM scans revealed abnormal grain growth above 36 000 and 21 600 s for 500°C and 530°C respectively, as mainly S grains (and also some Brass and Cu grains) grew massive. In order to understand the selection mechanisms of the abnormal grain growth, both the GBCD (measured with respect to ideal orientations) and grain size distributions (within 20° of individual orientations) were studied.

Figure 5(a) plots the number fraction of 1–10° and 10–20° boundaries which an ideal S, Brass, Cu, CG, H and CH orientation will have with the grains present in the 500°C/3 s annealed sample. Number fractions of such boundaries for ideal Goss orientation (which are not given in Fig. 5(a)) were observed to be similar to S/Brass/Cu. Grains outside these six orientations, and selected at random from the OIMs,

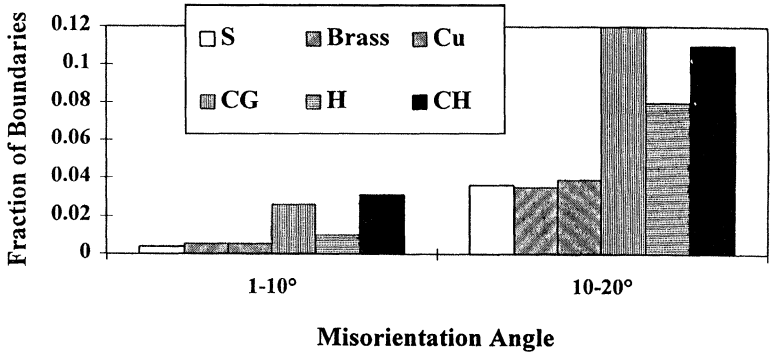

FIGURE 5(a) Fraction of boundaries within 1–10° and 10–20° with exact S, Brass, Cu, CG, H and CH orientations, as observed in 500°C/3 s annealed material.

showed values of boundary fractions similar to CG/H/CH. It should be noted that qualitatively *similar* trends of 1–10° and 10–20° boundary distributions were observed at other annealing temperatures and times as well. In other words, irrespective of the annealing conditions, S/Brass/Cu/Goss grains had the *lowest* probablities of encountering low angle boundaries. A growing grain can be stopped by particle pinning and/or by grains of similar orientation. Prolonged heating at 500°C/530°C may remove effects of particle pinning. But even in the absence of particle pinning, grains may be 'effectively' pinned and grain growth may be inhibited by low angle/low mobility boundaries. Lower probabilities for S/Brass/Cu/Goss grains to encounter low angle (and hence low mobility) boundaries might have played a role in their selection for abnormal grain growth.

Another role for GBCD may exist in the possible differences in the low energy, but high mobility, boundaries (e.g. low CSLs). Figure 5(b) plots the total number fraction of CSL boundaries ($\Sigma3$–$\Sigma29$) with ideal S, Brass, Cu, Goss, H and CH orientations in 500°C/3 s annealed sample. Fraction of CSL boundaries present among the matrix grains (i.e. among immediate neighbors) are also marked in the figure. As shown in the figure, the Cu/S/Brass/Goss had slightly higher probabilities of encountering/possessing CSL boundaries (mainly in terms of the low CSL boundaries of $\Sigma5$ and $\Sigma9$). Measurements at other annealing conditions also showed slight but consistently higher probabilities for ideal Cu/S/Brass/Goss orientations to possess low CSL ($\Sigma3$–$\Sigma9$) boundaries. Orientations with higher probabilities of possessing CSL boundaries may also be favored for abnormal grain growth (Rollett and Mullins, 1997).

Table II shows the average grain sizes for different orientations in 500°C/3 s and 3600 s annealed samples and Figs. 6(a) and (b) plot the observed grain size distributions. Values for average grains (i.e. irrespective of orientations) are also shown. In the initial microstructure (i.e. 500°C/3 s), typically a bimodal grain size distribution was observed. The relatively large fractions of small grains (responsible for such a bimodal size distribution) were possibly due to PSN, as discussed elsewhere (Samajdar *et al.*, 1997). Grain sizes of Cu and Goss were comparable with average grain sizes, while grains of S and Brass were *slightly* larger. At 3600 s (i.e. just before the initiation of abnormal grain growth), the number fraction of small grains decreased and grain

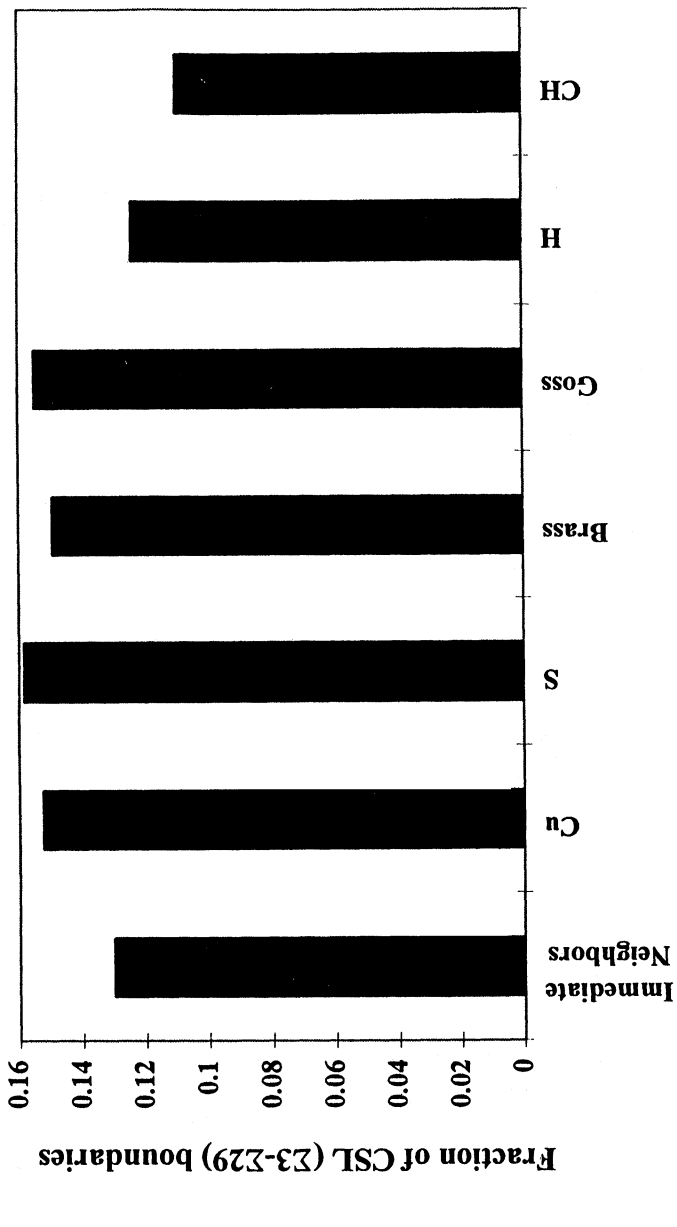

FIGURE 5(b) Fraction of CSL ($\Sigma 3$–$\Sigma 29$) boundaries with ideal S, Brass, Cu, Goss orientations, as observed in 500°C/3 s annealed material. Fraction of CSL of boundaries among matrix grains (i.e. with immediate neighbors) are also marked.

TABLE II Average grain size after annealing at 500°C for respectively 3 and 3600 s. Second column refers to all grains (irrespective of orientation) and the next columns refer to grains of specific orientations

Sample	*Average* (μm)	*Cu* (μm)	*Goss* (μm)	*Brass* (μm)	*S* (μm)
500°C, 3 s	4.35	4.5	4.37	4.96	5.23
500°C, 3600 s	6.81	8.0	7.7	8.7	9.4

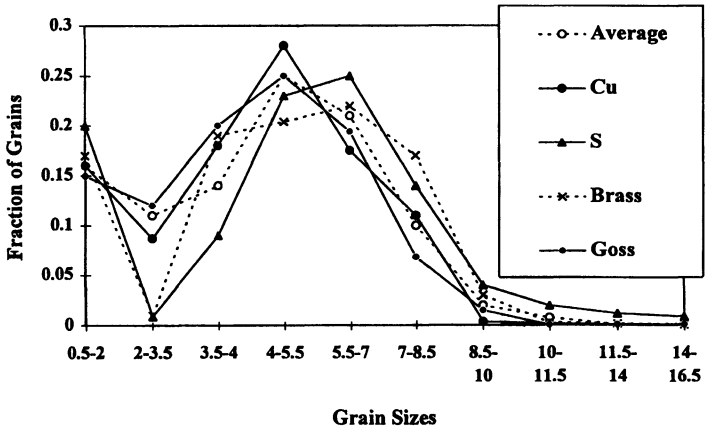

FIGURE 6(a) Number fraction of grains of different orientations (within 20° of the exact orientations) as a function of grain size in 500°C/3 s annealed material.

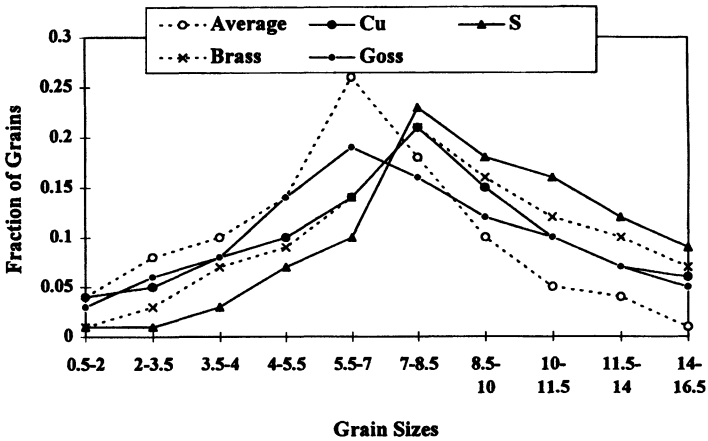

FIGURE 6(b) Number fraction of grains of different orientations (within 20° of the exact orientations) as a function of grain size in 500°C/3600 s annealed material.

size distributions shifted to higher values (see Fig. 6(b)). Interestingly enough, the shift in S/Brass/Cu/Goss was more than the shift in average grain sizes (which was true even for Cu and Goss which initially had similar to average grain size distributions, as shown in Fig. 6(a)).

DISCUSSION

I. Changes in Grain Size and GBCD with Annealing

Annealing may change grain sizes. However, in an alloy containing fine dispersoids (like the AA5182 of the present study), the grain size may be restricted by the Zener pinning, as the limiting grain size is expected to be $\{(4r)/(3F_v)\}$ (where r is the average dispersoid radius and F_v is the volume fraction) (Humphreys and Hatherly, 1995). Our approximate estimation, using backscattered electron imaging in SEM, showed the area fraction of dispersoids as 0.02. Assuming volume fraction and area fraction as similar and considering r as 0.1 μm, a limiting grain size of 6.7 μm is expected (which is close to our observed limiting grain size of 7–8 μm). After reaching the critical grain size, further grain growth was possible (at 500°C/530°C) only after dissolution/coarsening of the dispersoids, see Fig. 1.

Annealing and grain growth may change the GBCD, as boundary tensions may reduce the total amount of high energy boundaries (Humphreys and Hatherly, 1995). Computer modelling (Humphreys, 1992) and experimental studies (Randle and Brown, 1989; Watanabe *et al.*, 1989) have shown an increase in low angle and CSL boundaries with annealing. Our results indicate that in the commercial alloy AA5182, the total amount of extremely low angle (1–5°) boundaries increase quite dramatically with annealing. However, boundaries within 5–20° and also the CSL boundaries (Σ3–Σ29) did *not* change noticeably with annealing time/temperature, see Figs. 2 and 3. Increase in 1–5° boundaries was more at 470°C, when dispersoids were stable and grain boundaries were effectively pinned, that at 500°C/530°C, when limited grain growth was observed. If (i) boundary tension is primarily responsible for changes in GBCD (in our case increase in 1–5° boundaries) and (ii) pinned boundaries are more affected by boundary tension, then a combination of (i) and (ii) may explain our results. One may make such easy speculations and explain observed

trends in experimental results, but much remains to be learnt on the interaction of grain boundaries and dispersoids – especially when it may involve dissolution/coarsening.

II. Abnormal Grain Growth

Abnormal grain growth was observed after dispersoid dissolution/coarsening, as mainly S (and also some Brass and Cu) grains grew abnormally. Even in the starting as recrystallized microstructure (500°C/3 s annealed), the S and Brass grains were slightly larger than the average (see Table II). With further annealing, the size advantage increased. Grain size distributions for Cu/Goss were similar to that of average grains (see Table II and Fig. 6(a)). However, with subsequent annealing Cu/Goss grains gained a limited size advantage (as in Table II and Fig. 6(b)). Only a statistical approach to the grain size distributions (Abbruzzese and Lücke, 1986) may not be sufficient to explain such changes. Our observations on GBCD may indicate another possibility.

Considering the growth of an isolated grain, simple 2-dimensional modelling (Rollett and Mullins, 1997) has shown that high mobility and low boundary energy may promote abnormal grain growth. S/Brass/Cu/Goss grains had the lowest probability of encountering low angle/low mobility boundaries, but higher probability of possessing low energy/CSL boundaries, see Fig. 5. Such a combination may favor abnormal grain growth (Rollett and Mullins, 1997). It should be noted that the values reported in Fig. 5 are the average of the calculated values for all variants of ideal S/Brass/Cu/Goss orientations. S has four variants, while Brass/Cu/Goss have two each. Thus for a particular variant, especially for S, the probabilities of encountering low mobility or high energy boundaries may be lower or higher than the reported values of Fig. 5. Such lower/higher probabilities were observed locally for some, but not all, of the largest S grains. During abnormal grain growth, the final microstructure and texture is basically due to a few overgrown grains. Larger than average grain sizes for S (see Fig. 6) and also the fact that some of such large S grains may be favorably oriented/placed to encounter more of high mobility and low energy boundaries, possibly determined the orientation selection for abnormal grain growth in this material.

Grain boundary pinning by randomly distributed fine dispersoids may be obtained from Zener pinning pressure as $\{(3F_v\gamma)/(2r)\}$, where F_v and r are the volume fraction and average radius of the dispersoids and γ is the specific energy of the boundary with the dispersoids (Humphreys and Hatherly, 1995). For a low energy boundary (e.g. low CSL boundaries) γ and correspondingly the Zener pinning pressure is expected to be lower. In other words, a low CSL boundary may be less susceptible to dispersoid pinning. This may also explain the observation that growth of orientations (i.e. S/Brass/Cu/Goss), with slightly higher probability for encountering/possessing CSL boundaries, were somewhat favored (especially for Cu/Goss – which did not possess an initial size advantage (see Fig. 6 and Table II)). Experimental observations in Si–Fe (Harase and Shimuzu, 1988) had also shown that Goss grains may not possess a size advantage in the initial microstructure, but still may get selected for abnormal grain growth. Such a phenomenon was explained from the GBCD relationship between Goss and matrix and specific grain boundary migration characteristics associated with the particle pinning (Harase and Shimuzu, 1988). Our observations on the favored growth of S/Brass/Cu/Goss may follow the same logic.

CONCLUSIONS

(1) Limited grain growth to a critical grain size was observed immediately after primary recrystallization. Further grain growth was only possible after prolonged annealing at 500°C/530°C, which dissolved/coarsened the dispersoids responsible for grain boundary pinning.
(2) Prolonged annealing (from 30 to 21 600 s) was observed to increase the fraction of 1–5° boundaries. The increase was more at 470° (when grain growth was effectively arrested) than at 500°C/530°C (when limited grain growth was observed). However, the nature of the 5–20° and CSL boundaries did not change significantly with annealing.
(3) Abnormal grain growth was observed after 500°C/36 000 s and 530°C/21 600 s annealing, as mainly S (and also some brass and Cu) grains grew abnormally.

(4) In the starting as recrystallized microstructure, Brass and S grains had a slight size advantage. The size advantage improved with subsequent annealing. Interestingly enough, Cu and Goss grains (which did not have a size advantage in the starting as recrystallized microstructure) also gained limited size advantage during annealing.
(5) S/Brass/Cu/Goss grains had lower probabilities of encountering low angle boundaries, but higher probabilities for encountering/possessing CSL boundaries. These might have played a role in improving the size advantage for S/Brass, and for acquiring limited size advantage for Cu/Goss.
(6) Both the size advantage and GBCD possibly determined the selection mechanism for abnormal grain growth.

Acknowledgements

Financial support from FKFO grant no: G.0252.96 and supply of the rolled material from Hoogovens Aluminium are well appreciated. Part of the research was carried out in the frame of an European COST 512 action.

References

Abbruzzese, G. and Lücke, K. (1986). *Acta Metall.*, **34**(5), 905–914.
Brandon, D.G. (1966). *Acta Metall.*, **14**, 1479–1485.
Bunge, H.J. (1982). *Texture Analysis in Materials Science*, London: Butterworths.
Chiba, A., Handa, S., Watanabe, T., Abe, T. and Obana, T. (1994). *Acta Metall. Mater.*, **42**(5), 1733–1738.
Harase, J. and Shimuzu, R. (1988). *Trans. JIM*, **29**(5), 388–398.
Hayakawa, Y. and Szpunar, J.A. (1997). *Acta Mater.*, **45**(3), 1285–1295.
Humphreys, F.J. (1992). *Scripta Metall.*, **27**, 1557–1562.
Humphreys, F.J. and Hatherly, M. (1995). *Recrystallization and Related Annealing Phenomena*, UK: Elsevier Sci. Ltd.
Palumbo, G., King, P.J., Aust, K.T., Erb, U. and Lichtenberger, P.C. (1991). *Scripta Metall. Mater.*, **25**, 1775–1780.
Rabet, L. (1996). Ph.D. Thesis (in Dutch), ISBN No: 90-5682-021-4, Katholieke Universiteit Leuven, Belgium.
Randle, V. and Brown, A. (1989). *Phil. Mag. A*, **59**(5), 1075–1089.
Randle, V. (1992). *Microtexture Determination and its Application*, London: The Inst. of Mater.
Ratchev, P., Verlinden, B. and Van Houtte, P. (1995). *Acta Metall. Mater.*, **43**(2), 621–629.
Rollett, A.D. and Mullins, W.W. (1997). *Scripta Mater.*, **36**(9), 975–980.
Samajdar, I. and Doherty, R.D. (1994). *Scripta Metall. Mater.*, **31**(5), 527–530.
Samajdar, I., Rabet, L., Verlinden, B. and Van Houtte, P. (1997). Submitted to the special issue on recrystallization in ISIJ (1998).

Smith, D.A. and Pond, R.C. (1976). *Int. Metals Rev.*, **21**, 61–74.
Van Houtte, P. (1995). *MTM-FHM software and Manual, Version 2*, ed. MTM-KULeuven, Belgium.
Watanabe, T., Fujii, H., Oikawa, H. and Arai, K.I. (1989). *Acta Metall.*, **37**, 941–952.
Watanabe, T. (1992). *Scripta Metall. Mater.*, **27**, 1497–1502.